# Ultrasensitive second-harmonic generation frequency-resolved optical gating by aperiodically poled LiNbO$_3$ waveguides at 1.5 $\mu$m

**Shang-Da Yang and Andrew M. Weiner**

*Purdue University, West Lafayette, Indiana 47907*

**Krishnan R. Parameswaran**

*JDS Uniphase, Santa Rosa, California 95407*

**Martin M. Fejer**

*E. L. Ginzton Laboratory, Stanford University, Stanford, California 94305*

We retrieve intensity and phase profiles of 280 fs, 50 MHz optical pulses with 124 aJ coupled pulse energy (960 photons) by second-harmonic generation (SHG) frequency-resolved optical gating, using aperiodically poled LiNbO$_3$ waveguides. The strong nonlinear interaction that is due to confinement within the micrometer-sized waveguide structure and the linearly chirped poling period contribute, respectively, to high SHG efficiency and broad phase-matching bandwidth. The achieved sensitivity is $2.7 \times 10^{-6}$ mW$^2$, improving on the previous record for self-referenced complete pulse characterization by 5 orders of magnitude.    © 2005 Optical Society of America

*OCIS codes:* 320.7100, 320.7110, 130.3730.

The comprehensive applications of ultrafast optics rely largely on the ability of fully characterizing the ultrashort ($10^{-12}$–$10^{-15}$ s) signal pulses, especially when nearly bandwidth-limited or precisely shaped pulses are involved, such as those in high-bit-rate telecommunication transmissions,[1] optical code-division multiple-access systems,[2] and nonlinear-optical material characterizations. To meet the requirements of limited power budgets in optical communication systems and weak ($<10^{-15}$ J) signal pulses in material characterization, several sensitive schemes have been proposed for complete intensity and phase characterization of ultrashort pulses. For example, temporal analysis by dispersing a pair of light *E* fields (TADPOLE) has been demonstrated to measure near-infrared pulses at 42 zeptojoules ($42 \times 10^{-21}$ J) per shot,[3] and a linear spectrogram technique that uses electroabsorption temporal gating permits measurement of telecommunication pulses at 10 attojoules ($10^{-17}$ J).[4] However, the former requires a strong, synchronized, and well-characterized optical reference, while the latter is limited to ~3 ps temporal resolution and requires a synchronized electronic clock. Within the regime of self-referenced measurements, four-wave mixing in a semiconductor optical amplifier and in a 22 km long dispersion-shifted fiber have been employed for quadratic frequency-resolved optical gating (FROG) measurements with sensitivities (defined as the peak power–average power product for the minimum detectable input) of 50 and 0.2 mW$^2$, respectively,[5,6] improving on the conventional SHG FROG measurements that use bulk crystals by 1–3 orders of magnitude.[1] In addition to the extra requirement of a continuous-wave pump and limitation of the picosecond-order mini-

mum measurable pulse durations, the resultant sensitivities of these four-wave mixing approaches still do not meet the requirement for microwatt-order average powers for monitoring optical communication systems.[1] Recently we reported that intensity autocorrelation measurements by SHG with aperiodically poled lithium niobate (A-PPLN) waveguides are much more sensitive than other existing techniques and demonstrated autocorrelations of 220 fs optical pulses at a 50 MHz repetition rate and 52 aJ energy per pulse, corresponding to a record sensitivity of $3.2 \times 10^{-7}$ mW$^2$.[8] Here we utilize the A-PPLN waveguide for the more sophisticated SHG FROG technique that permits complete pulse retrieval. We achieve a sensitivity of $2.7 \times 10^{-6}$ mW$^2$, nearly 5 orders of magnitude better than the previously reported.[6]

Figure 1 shows a schematic diagram of our experiments. We use a passively mode-locked fiber laser plus a bandpass filter to produce laser pulses with ~280 fs duration, a 50 MHz repetition rate, and 1538 nm central wavelength. The pulse train is sent into a collinear-type free-space Michelson interferometer (MI) to produce pulse pairs with variable delay $\tau$
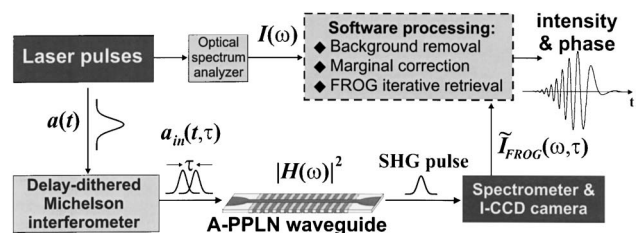


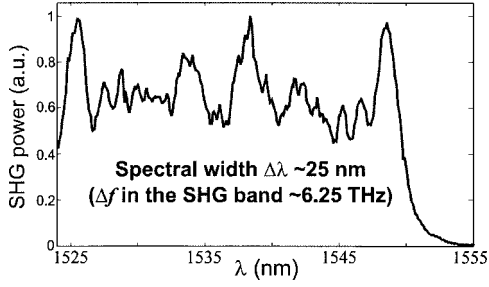Fig. 1. Schematic diagram of the experimental setup: I-CCD, intensified charge-coupled device.

Fig. 2.  Phase-matching tuning curve of the A-PPLN wave-guide measured at 21°C.

that are coupled into an A-PPLN waveguide with ~6 cm long poling region to produce a SHG signal.[8] A spectrometer and an intensified CCD camera are employed to record the SHG power spectrum for each delay $\tau$, which yields the raw FROG trace $\tilde{I}_{\mathrm{FROG}}(\omega, \tau)$.

The complex field envelope of the pulse pair from the MI can be characterized as $a_{\mathrm{in}}(t, \tau) \equiv a(t) + a(t - \tau) \times \exp(-j\omega_0\tau)$, where $a(t)$ indicates the input field envelope and $\omega_0$ is the carrier's angular frequency. The induced nonlinear polarization spectrum $P_{\mathrm{NL}}(\omega, \tau) = \mathrm{FT}\{a_{\mathrm{in}}^2(t, \tau)\}$ (where FT is Fourier transform) will contain unwanted interferometric fringes:

$$P_{\mathrm{NL}}(\omega, \tau) P_{\mathrm{NL}}^{(\mathrm{X})}(\omega, 0) \times \{1 + \exp[-j(\omega + 2\omega_0)\tau]\}$$
$$+ 2P_{\mathrm{NL}}^{(X)}(\omega, \tau) \times \exp(-j\omega_0\tau). \quad (1)$$

$P_{\mathrm{NL}}^{(X)}(\omega, \tau) \equiv \mathrm{FT}\{a(t) \times a(t - \tau)\}$ is the self-gated nonlinear polarization spectrum. We dither one of the interferometer arms by a few optical wavelengths at 180 Hz to average out the interferometric fringes. The resultant averaged nonlinear polarization power spectrum $|\bar{P}_{\mathrm{NL}}(\omega, \tau)|^2$ consists of only the background and gating terms:

$$|\bar{P}_{\mathrm{NL}}(\omega, \tau)|^2 \propto |P_{\mathrm{NL}}^{(\mathrm{X})}(\omega, 0)|^2 + 2|P_{\mathrm{NL}}^{(X)}(\omega, \tau)|^2, \quad (2)$$

where $|P_{\mathrm{NL}}^{(X)}(\omega, \tau)|^2$ is the standard noncollinear SHG FROG trace $I_{\mathrm{FROG}}(\omega, \tau)$. Compared with $|\bar{P}_{\mathrm{NL}}(\omega, \tau)|^2$ in relation (2), the raw FROG trace $\tilde{I}_{\mathrm{FROG}}(\omega, \tau)$ is generally modulated by the phase-matching response $|H(\omega)|^2$ of the SHG crystal[9]:

$$\tilde{I}_{\mathrm{FROG}}(\omega, \tau) \propto |\bar{P}_{\mathrm{NL}}(\omega, \tau) \times H(\omega)|^2$$
$$= [|I_{\mathrm{FROG}}(\omega, 0) + 2|I_{\mathrm{FROG}}(\omega, \tau)] \times |H(\omega)|^2, \quad (3)$$

where $H(\omega)$ is associated with the nonlinear coefficient $d_{\mathrm{eff}}(z)$ of the SHG crystal through a Fourier transform relation.[10] For thick uniform bulk crystals [$d_{\mathrm{eff}}(z)$ is constant] and long unchirped periodically poled lithium niobate (PPLN) waveguides [$d_{\mathrm{eff}}(z)$ is strictly periodic], $|H(\omega)|^2$ is a sinc$^2$ curve with a narrow bandwidth, $\Delta f$ (e.g., $\Delta f \sim 43$ GHz in the SHG band for a 6-cm-long PPLN guide). This may filter out the desired spectral information. In the A-PPLN waveguide scheme we can broaden $|H(\omega)|^2$

and almost completely preserve the SHG pulse yield by linearly chirping the poling period [$d_{\mathrm{eff}}(z)$ has a longitudinally varying period].[8] As shown in Fig. 2, the phase-matching (PM) tuning curve (normalized SHG power as a function of input wavelength) of our A-PPLN waveguide is ~25 nm wide, sufficiently broad to cover the FROG trace of 280 fs pulses. However, it presents oscillatory features that are due to the imperfect apodization of $d_{\mathrm{eff}}(z)$, which acts as a spectral distortion $|H(\omega)|^2$ in relation (3). To eliminate $|H(\omega)|^2$, we subtract a spectrum taken at a large delay from the raw trace $\tilde{I}_{\mathrm{FROG}}(\omega, \tau)$ to get a background-free trace $\tilde{I}_{\mathrm{FROG}}'(\omega, \tau) \propto I_{\mathrm{FROG}}(\omega, \tau) \times |H(\omega)|^2$ and then apply the frequency marginal correction technique[11]:

$$I_{\mathrm{FROG}}(\omega, \tau) \propto \{\tilde{I}_{\mathrm{FROG}}'(\omega, \tau) \times [I(\omega)$$
$$\otimes I(\omega)]\} \bigg/ \left[ \int \tilde{I}_{\mathrm{FROG}}'(\omega, \tau)\mathrm{d}\tau \right], \quad (4)$$

where $I(\omega)$ is the input power spectrum measured by an optical spectrum analyzer and $\otimes$ stands for convolution. Subsequently, we employ commercial software (Femtosoft FROG) to completely retrieve the intensity and phase of the pulses. Our FROG trace acquisition uses 800 ms exposure for each delay step, taking ~135 s for a scanning range of 2.6 ps with 20 fs delay increments. The retrieval process normally converges within 1 min.

Figure 3 illustrates measured and retrieved FROG traces $I_{\mathrm{FROG}}(\omega, \tau)$ (grid size, $64 \times 64$) by use of nearly bandwidth-limited pulses with coupled pulse energies of 9.5 fJ [Figs. 3(a) and 3(b)] and 124 aJ [Figs. 3(c) and 3(d)]. The latter energy is equivalent to 0.44 mW peak power and 6.2 nW average power, corresponding to an unprecedented FROG sensitivity of $2.7 \times 10^{-6}$ mW$^2$. Even with a 19 dB input power difference (38 dB difference for SHG powers), these FROG traces agree well with one another. The FROG errors (rms deviation between measured and retrieved traces) are 0.0022 and 0.0032, respectively. Figure 4 shows the retrieved pulses in the frequency [Fig. 4(a)] and the time [Fig. 4(b)] domains for both input power levels. An independently measured input power spectrum is plotted as a dotted curve in Fig. 4(a) for comparison. The retrieved spectral inten-
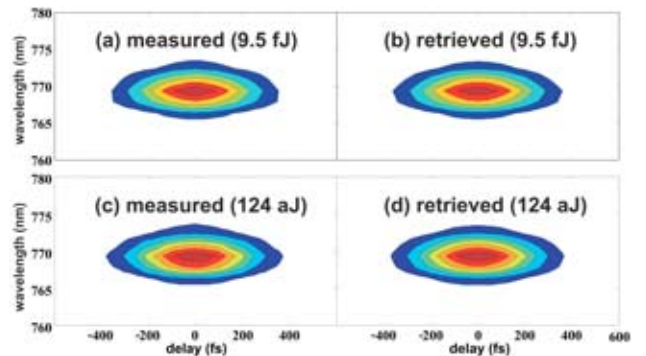


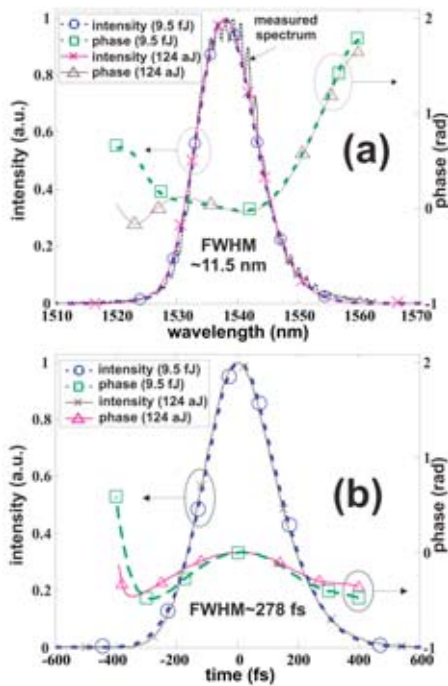Fig. 3.  Measured and retrieved FROG traces.

Fig. 4.   Retrieved pulse depicted in (a) the frequency domain and (b) the time domain for both 9.5 fJ and 124 aJ coupled pulse energies. The dotted curve in (a) represents the independently measured power spectrum.
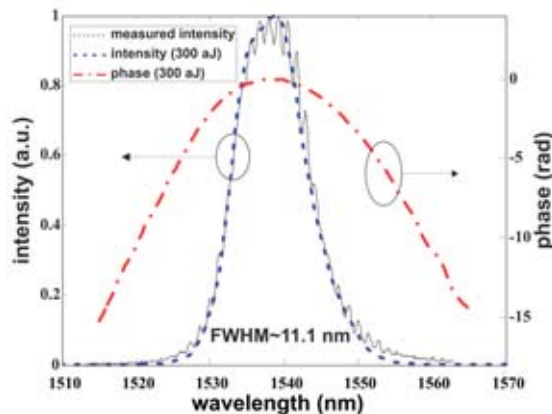


Fig. 5.   Retrieved spectral intensity and phase of the pulse dispersed by a 5 m long SMF. The pulse dispersion is estimated as −70 fs/nm.

sities closely approach this curve, except for the oscillatory fine structure, which arises from the interference between the main pulse and an attenuated replica caused by reflections at the bandpass filer. Better spectral resolution and a larger delay scanning range would be required for resolution of these features in the measurement. The retrieved temporal profiles also overlap well and have similar intensity FWHM values: 279 and 278 fs, respectively (time-reversal ambiguity exists as usual in SHG FROG).

To further verify the measurement capability, we inserted a section of 5 m long single-mode fiber (SMF) into the link to increase the quadratic spectral phase and performed the FROG measurement. The retrieved spectral intensity and phase profiles with coupled energy of 300 aJ per pulse are shown in Fig. 5. The spectral phase is predominantly parabolic; the anomalous dispersion of SMF uniquely determines the sign of the retrieved spectral phase. Fitting the spectral phase profile shows that the quadratic phase coefficient is $-4.36 \times 10^{-2}$ ps$^2$. Disregarding the small chirp measured in Fig. 4 ($\sim 2.60 \times 10^{-2}$ ps$^3$, while the sign is ambiguous), we estimated that the 5 m long SMF introduces an accumulated dispersion of −70 fs/nm, close to the value predicted by the SMF specification (−83 fs/nm) near the 1538-nm band. The retrieved temporal FWHM is broadened to ∼800 fs, also in good agreement with that predicted by the measured spectral width and dispersion.

In conclusion, we have applied a chirped A-PPLN waveguide to make ultrasensitive SHG FROG pulse measurements at nanowatt average power. The sensitivity is $2.7 \times 10^{-6}$ mW$^2$, substantially improving on the previous record by 5 orders of magnitude. This asynchronous technique can be applied to optimizing high-bit-rate transmitters,[1] monitoring 10-Gbit/s signal pulses at practical submicrowatt average power levels,[7] and providing detailed pulse information for precise field control.

**References**

1. B. C. Thomsen, D. A. Reid, R. T. Watts, L. P. Barry, and J. D. Harvey, IEEE Trans. Instrum. Meas. **53**, 186 (2004).
2. Z. Jiang, D. S. Seo, S.-D. Yang, D. E. Leaird, R. V. Roussev, C. Langrock, M. M. Fejer, and A. M. Weiner, J. Lightwave Technol. **23**, 143 (2005).
3. D. N. Fittinghoff, J. L. Bowie, J. N. Sweetser, R. T. Jennings, M. A. Krumbugel, K. W. DeLong, R. Trebino, and I. A. Walmsley, Opt. Lett. **21**, 884 (1996).
4. C. Dorrer and I. Kang, Opt. Lett. **27**, 1315 (2002).
5. P.-A. Lacourt, M. Hanna, and J. M. Dudley, IEEE Photonics Technol. Lett. **17**, 157 (2005).
6. P.-A. Lacourt, J. M. Dudley, J-M. Merolla, H. Porte, J.-P. Goedgebuer, and W. T. Rhodes, Opt. Lett. **27**, 863 (2002).
7. M. Dinu and F. Ouochi, J. Opt. Networking **1**, 237 (2002).
8. S.-D. Yang, A. M. Weiner, K. R. Parameswaran, and M. M. Fejer, Opt. Lett. **29**, 2070 (2004).
9. A. Baltuska, M. S. Pshenichnikov, and D. A. Wiersma, Opt. Lett. **23**, 1474 (1998).
10. G. Imeshev, M. A. Arbore, M. M. Fejer, A. Galvanauskas, M. Fermann, and D. Harter, J. Opt. Soc. Am. B **17**, 304 (2000).
11. R. Trebino, K. W. DeLong, D. N. Fittinghoff, J. N. Sweetser, M. A. Krumbugel, and D. J. Kane, Rev. Sci. Instrum. **68**, 3227 (1997).